Nutrition
Research and
Practice

Original Research

Check for updates

Protective effects of red orange (*Citrus sinensis* [L.] Osbeck [Rutaceae]) extract against UVA-B radiation-induced photoaging in Skh:HR-2 mice

Yoon Hee Kim [1*], Cho Young Lim [1*], Jae In Jung [2], Tae Young Kim [1], and Eun Ji Kim [2§]

[1]Technology Development Center, BTC Corporation, Ansan 15588, Korea
[2]Industry Coupled Cooperation Center for Bio Healthcare Materials, Hallym University, Chuncheon 24252, Korea

§**Corresponding Author:**
Eun Ji Kim
Industry Coupled Cooperation Center for Bio Healthcare Materials, Hallym University, 1 Hallymdaehak-gil, Chuncheon 24252, Korea.
Tel. +82-33-248-3106
Fax. +82-33-244-3107
Email. myej4@hallym.ac.kr

*Yoon Hee Kim and Cho Young Lim contributed equally to this work.

ORCID iDs
Yoon Hee Kim
https://orcid.org/0000-0002-6045-9927
Cho Young Lim
https://orcid.org/0000-0002-2171-6847
Jae In Jung
https://orcid.org/0000-0002-4475-1434
Tae Young Kim
https://orcid.org/0000-0003-1428-1176

ABSTRACT

BACKGROUND/OBJECTIVES: The skin is the outermost organ of the human body and plays a protective role against external environmental damages, such as sunlight and pollution, which affect anti-oxidant defenses and skin inflammation, resulting in erythema or skin reddening, immunosuppression, and epidermal DNA damage.
MATERIALS/METHODS: The present study aimed to investigate the potential protective effects of red orange complex H extract (ROC) against ultraviolet (UV)-induced skin photoaging in Skh:HR-2 mice. ROC was orally administered at doses of 20, 40, and 80 mg/kg/day for 13 weeks, along with UV irradiation of the mice for 10 weeks.
RESULTS: ROC improved UV-induced skin barrier parameters, including erythema, melanin production, transepidermal water loss, elasticity, and wrinkle formation. Notably, ROC inhibited the mRNA expression of pro-inflammatory cytokines (interleukin 6 and tumor necrosis factor α) and melanogenesis. In addition, ROC recovered the UV-induced decrease in the hyaluronic acid and collagen levels by enhancing genes expression. Furthermore, ROC significantly downregulated the protein and mRNA expression of matrix metalloproteinases responsible for collagen degradation. These protective effects of ROC against photoaging are associated with the suppression of UV-induced phosphorylation of c-Jun NH2-terminal kinase and activator protein 1 activation.
CONCLUSIONS: Altogether, our findings suggest that the oral administration of ROC exerts potential protective activities against photoaging in UV-irradiated hairless mice.

Keywords: Skin aging; collagen; erythema; matrix metalloproteinases; hyaluronic acid

INTRODUCTION

The skin is the first protective barrier against external environmental stressors, such as solar ultraviolet (UV) radiation, air pollution, smoking, nutrition, and cosmetic products, which may compromise skin integrity [1]. Skin aging can be classified into chronological aging, a process that occurs as a result of the passage of time, and extrinsic aging or photoaging,

Eun Ji Kim
https://orcid.org/0000-0001-9305-4769

which is caused by prolonged sun exposure, particularly to UV radiation (UVR), such as UVA and UVB. The injurious effects of skin photoaging are caused by excessive exposure to UVR and are manifested as rough, dry, and sagging skin, deep wrinkles, laxity, excessive skin pigmentation, or skin cancers [2-5].

UVR consists of 3 wavelength regions: UVA (λ = 320–400 nm), UVB (λ = 280–320 nm), and UVC (λ = 100–280 nm) [6]. Excessive exposure to UVR can produce physiological responses and damage skin structures by generating reactive oxygen species. This in turn stimulates the mitogen-activated protein kinase (MAPK) family is stimulated. MAPKs are divided into extracellular signal-regulated kinase 1/2 (ERK1/2), c-Jun NH2-terminal kinase (JNK), and p-38 kinases. ERK1/2 activation by mitogenic signals stimulates cell proliferation and differentiation and is involved in tumorigenesis stimulation by oxidative stress. The phosphorylation of JNK and p-38, activated by DNA-damaging environmental stressors, such as UVR, inflammatory cytokines, and heat shock, participates in cellular differentiation and inflammatory responses. The activation of 2 nuclear transcription factors, activator protein 1 (AP-1), and nuclear factor-κB (NF-κB), is related to the transcription of genes that degrade enzymes of the dermal extracellular matrix (ECM) and inflammatory cytokines, respectively. These transcription factors are connected to various molecular signaling pathway changes in the dermis and epidermis, leading to disrupted anti-oxidant defenses, skin dryness, pigmentation, breakdown of extracellularly synthesized collagen, deep wrinkling, and apoptosis activation [7,8].

The most common approach to protect skin from photoaging is the topical application of sunscreens, which is measured by the sun protection factor (SPF) and shows the potential ability to prevent sunburn. Nevertheless, the relatively low SPF consisting of titanium dioxide and zinc oxide have been reported for UV stability and toxicity to humans and the environment [9]. Recently, there has been growing awareness of the beneficial effects of oral photoprotection, associated with skin health, and several phytochemicals have transpired as a positive alternative strategy to prevent and alleviate the damage caused by photoaging [10].

Citrus sinensis (L.) Osbeck (Rutaceae), known as red orange, is rich in polyphenols and ascorbic acid, and has a strong anti-oxidant profile. In fact, the anti-oxidant activity of red orange extract, which is highly concentrated in anthocyanins, hydroxycinnamic acids, flavanones, and vitamin C, has been extensively studied in different target populations of athletes, diabetics, smokers, and subjects exposed to air pollution [11-15]. The skin-protective properties of this extract against erythema and hyperpigmentation, induced by sunlamp exposure, have also been extensively investigated. In a previous study, red orange complex H extract (ROC) was administered to examine its protective effect against UVA-B-induced damage and was found to increase the scavenger activity, UVB protection, and anti-inflammatory properties by activating tumor necrosis factor (TNF)-α, interleukin (IL)-6, and NF-κB, and downregulating matrix metalloproteinases (MMPs) content *in vitro* [16]. Furthermore, the results of several clinical studies have evidenced that ROC exerts photoprotective and anti-aging effects [17].

Although the beneficial effects of ROC have been confirmed, the molecular mechanisms of their protective effects during UVR in mice remain unclear. Therefore, in the present study, we examined the effects of the oral administration of ROC on the principal skin damage of UV-induced hairless mice. Specifically, the following potential mechanisms of ROC protective effects were explored: (1) pro-inflammation response, including the secretion

of proinflammatory factors such as IL-6 and TNF-α; (2) inhibition of skin pigmentation via changes in the melanin content; (3) enhancing skin moisturizing (alterations in the hyaluronic acid [HA] content and hyaluronic acid synthase [HAS] activities); and (4) suppression of wrinkle formation (via changes int collagen synthesis and MMP expression). The obtained results were expected to provide evidence of potential ROC protection mechanisms against UVR-induced skin aging.

MATERIALS AND METHODS

Preparation of the standardized ROC

ROC (batch number 03202004-01) was obtained from the juice of 3 red-orange (*C. sinensis* [L.] Osbeck) cultivars, Moro, Sanguinello, and Tarocco. Commercially available ROC® H (Bionap S.r.l, Belpasso, Italy) was obtained according to the established and patented manufacturing process. This complex was standardized to the content (w/w) of the following bioactive constituents by HPLC-DAD analysis: 2.2% ferulic acid, 0.4% narirutin, 9.0% hesperidin (9.4% total flavanones), 3.1% cyanidin 3-O-glucoside, and 6.5% ascorbic acid, except for cyanidin-3-O-glucoside, which was quantified using UV spectroscopy [16].

Ethical statement and animals

All animal experiments were conducted in compliance with the protocols approved by the Institutional Animal Care and Use Committee of Hallym University (Hallym 2020-20).

Five-week-old male Skh:HR-2 mice were purchased from DooYeol Biotech Co. Ltd. (Seoul, Korea). The mice were housed at the animal research facility of Hallym University and maintained under controlled standard conditions: $23 \pm 3°C$, $50 \pm 10\%$ relative humidity, 10–15 ventilations/h, 150–200 lx illumination, and 12-h light/dark cycles. The mice were provided with a commercial non-purified rodent diet (Cargil Agri Purina, Inc., Seongnam, Korea) and drinking water *ad libitum*.

UVA-B irradiation

UVA-B irradiation was performed with a UV irradiator (UV1-1000; BoTeck, Gunpo, Korea), which uses a UVA-B lamp (GL20SE; Sankyo Denki, Yokohama, Japan) as a light source that emits a 1:1 ratio of UVA at 315–400 nm (peak at 365 nm) and UVB at 280–315 nm (peak at 306 nm).

Effect of ROC administration on the minimum erythema dose (MED) of the dorsal skin

After a one-week adaptation period, Skh:HR-2 mice were randomly assigned into 4 groups (5 mice per group) as follows: (i) control group (vehicle-administered group, CON); (ii) 20 mg/kg body weight (BW)/day ROC-administered group (R20); (iii) 40 mg/kg BW/day ROC-administered group (R40); and (iv) 80 mg/kg BW/day ROC-administered group (R80). All mice were subjected to oral gavage with vehicle (distilled water) or ROC (20, 40, or 80 mg/kg BW/day) for 13 weeks. Thereafter, UVA-B irradiation was conducted to evaluate the effect of ROC administration on MED in the dorsal skin. The backs of the mice were divided into 6 sections (1×1 cm^2 each), and series of UVA-B irradiation doses of 30, 50, 70, 90, 120, and 150 mJ/cm^2 were applied. After 24-h UVA-B irradiation, the lowest dose at which erythema with clearly defined borders at 4 edges was observed was defined as the MED. Post-MED measurement, the mice were anesthetized with tribromoethanol diluted in tertiary amyl alcohol. Then, blood was collected from the orbital vein, and serum was obtained by centrifugation.

Effect of ROC administration on UVA-B-induced photoaging

After a one-week adaptation period, Skh:HR-2 mice were randomly divided into 5 groups (ten mice per group) as follows: (i) normal control group (without UV irradiation, vehicle-administered group, NOR); (ii) UV-irradiated control group (UV-irradiated, vehicle-administered group, UV + C); (iii) UV-irradiated and 20 mg/kg BW/day ROC-administered group (UV + R20); (iv) UV-irradiated and 40 mg/kg BW/day ROC-administered group (UV + R40); and (v) UV-irradiated and 80 mg/kg BW/day ROC-administered group (UV + R80). All mice were subjected to oral gavage with vehicle (distilled water) or ROC (20, 40, or 80 mg/kg BW/day) for 13 weeks. Before the initiation of UV irradiation, we measured the MED of the dorsal skin using the aforementioned method, and 50 mJ/cm^2 was determined to be equal to 1 MED. After 3-week ROC administration, the mice were exposed to UVA-B irradiation 3 times per week for ten weeks as follows: weeks 4–5 (based on the start date of ROC administration), 1 MED (50 mJ/cm^2); weeks 6–7, 2 MED (50 mJ/cm^2); and weeks 8–13, 3 MED (150 mJ/cm^2). At the end of the experimental period, mice were anesthetized with tribromoethanol diluted in tertiary amyl alcohol, and blood and dorsal skin specimens were immediately collected for analysis.

Evaluation of the parameters employed for skin quality assessment

One day before the end of the experiment, the erythema index, melanin index, transepidermal water loss (TEWL), elasticity index, and wrinkle index were evaluated to determine whether ROC administration improves skin quality. Skin erythema and melanin indices were measured using Mexameter® MX18 (Courage-Khazaka Electronic GmbH, Köln, Germany). The TEWL and elasticity indices were measured with a Corneometer® CM825, Tewameter® TM300, and Cutometer® MPA580 (Courage-Khazaka Electronic GmbH, Cologne, Germany), respectively. To evaluate wrinkle formation, skin replicas were cast on the dorsal skin surface of mice using SILFLO (Flexico Developments Ltd., Tokyo, Japan) and measured with a Visionmeter SV600 (Courage-Khazaka Electronic GmbH). The topography of the skin surface was then analyzed to determine its total roughness (the distance between the highest peak and the lowest value, R1), average roughness (the average of the 5 maximum distances, R2), maximum roughness (the largest value of the 5 maximum distances, R3), smoothness depth (R4), and arithmetic average roughness (R5).

Biochemical serum analyses

The levels of glucose, triglycerides, total cholesterol, blood urea nitrogen, creatinine, alanine aminotransferase, and aspartate aminotransferase in the serum were measured using a blood biochemistry analyzer (KoneLab 20XT; Thermo Fisher Scientific, Vantaa, Finland).

Histology and immunofluorescence (IF) staining

Dorsal skin tissues were fixed in 4% paraformaldehyde immediately after removal. The fixed skin tissues were embedded in paraffin, sectioned into 5-μm-thick slices, deparaffinized with xylene, and rehydrated using xylene and graded alcohol. To observe the changes in the melanin content in the skin tissue, Fontana-Masson's silver (Abcam, Cambridge, UK) staining was performed following the manufacturer's instructions. In addition, to investigate collagen 1 expression, IF staining was conducted with a primary antibody (collagen 1; Abcam) and fluorochrome-conjugated secondary antibody (anti-rabbit IgG-Alexa-488; Thermo Fisher Scientific). Nuclei were counterstained with 4',6-diamidino-2-phenylindole (Sigma-Aldrich, St. Louis, MO, USA). The stained slides were examined in a blind manner, and randomly chosen fields were photographed under a Carl Zeiss Axio Imager microscope (Carl Zeiss, Jena, Germany).

Measurement of the melanin content

The melanin content in the skin was measured as described previously [18]. Briefly, skin tissues were homogenized in lysis buffer (1 N NaOH) and heated at 80℃ for 1 h. The absorbance of the melanin extracted from the skin homogenate was then measured at 405 nm. The melanin content in each test group was expressed as a percentage of that in the NOR group.

Enzyme-linked immunosorbent assay (ELISA)

Skin tissues were homogenized in phosphate-buffered saline and centrifuged at 5,000 rpm for 10 min. The supernatant was collected and subjected to ELISA. The protein content of the supernatant was measured using a bicinchoninic acid (BCA) protein assay kit (Thermo Scientific, Rockford, IL, USA). The levels of HA (R&D Systems, Minneapolis, MN, USA), collagen (Abcam), IL-6 (R&D Systems), and TNF-α (R&D Systems) in skin homogenates were measured using the relevant ELISA kits according to the manufacturer's instructions.

Measurement of AP-1 content

Nuclear proteins from the skin tissues were extracted with a nuclear fraction kit (Abcam) following the manufacturer's instructions. The AP-1 content in the nuclear protein was next measured using an AP-1 ELISA kit (MyBioSource, San Diego, CA, USA).

Western blot analysis

Skin tissues were lysed as previously described [19]. The protein content of the lysates was measured using a BCA protein assay kit (Thermo Scientific). Western blot analyses were performed as reported earlier [20]. The antibodies used in this study were obtained from the following suppliers: MMP-3 and MMP-9 from Abcam and phospho-JNK (Thr183/Tyr185), JNK, and β-actin from Cell Signaling Technology (Beverly, MA, USA). Each protein band was visualized by an enhanced chemiluminescence method using Luminata™ Forte Western HRP Substrate (Millipore, Billerica, MA, USA). Relative protein expression was estimated using an ImageQuant™ LAS 500 imaging system (GE Healthcare Bio-Science AB, Uppsala, Sweden) and normalized to β-actin levels.

Quantitative real-time reverse transcription-polymerase chain reaction (RT-PCR)

Total RNA was isolated from skin tissues, and real-time RT-PCR was performed using a Rotor-Gene™ SYBR Green kit (Qiagen, Valencia, CA, USA) and Rotor-Gene 3000 PCR (Corbett Research, Mortlake, Australia), as described previously [19]. Information regarding the primer sequences used in this study is presented in **Supplementary Table 1**. The results were analyzed using the Rotor-Gene 6000 series System Soft program version 6 (Corbett Research). The relative expression of the target mRNA was normalized to that of glyceraldehyde 3-phosphate dehydrogenase.

Statistical analysis

All results are expressed as mean ± standard error of the mean (SEM). Statistical analyses were performed using the Statistical Analysis System for Windows version 9.4 (SAS Institute, Cary, NC, USA). The Student's *t*-test was employed to test the differences between the NOR and UV groups. Analysis of variance followed by Duncan's multiple comparison test was used to compare the means between the treatment groups. Statistical significance was set at $P < 0.05$.

RESULTS

ROC effects on MED in UVA-B-irradiated hairless mice

Skh:HR-2 mice were subjected to ROC for 13 weeks and irradiated with UVR (30, 50, 70, 90, 120, and 150 mJ/cm²). After 24 h, the MED of UV irradiation was determined (**Fig. 1**). A statistically significant increase in MED compared to CON (42.0 ± 4.9) was observed after 13 weeks of ROC administration. The means of MED were 74 ± 4.0 at R20, 92.0 ± 4.0 at R40, and 144.0 ± 6.0 at R80, showing a progressive enhancement of the UVR minimum dose required for erythema induction. For 13 weeks, mice were subjected to oral gavage with ROC 20, 40, or 80 mg/kg BW/day. Based on our previous clinical study results, 100 mg/day of ROC was defined as the effective anti-photoaging dosage. This was converted to a mice dose of 20, 40, or 80 mg/kg by the human equivalent dose [17,21]. Changes in BW and serum clinical parameters were measured to determine the toxicity of ROC (**Table 1**). There were no significant differences in BW or serum biochemical indicators between the groups. Therefore, ROC did not produce any significant toxic effect in mice during the 13-week period of the treatment.

Table 1. Effects of red orange complex H extract on the body weight and serum clinical parameters in Skh:HR-2 hairless mice

Variables	CON	R20	R40	R80
Initial body weight (g)	26.6 ± 0.4	26.9 ± 0.6	26.4 ± 0.8	26.8 ± 1.0
Final body weight (g)	32.7 ± 1.0	32.8 ± 1.7	32.5 ± 1.9	32.8 ± 2.3
Body weight gain (g)	6.1 ± 0.1	5.9 ± 0.4	6.0 ± 0.2	6.0 ± 0.3
Glucose (mg/dL)	2,483.1 ± 8.8	242.8 ± 7.6	230.1 ± 9.5	243.4 ± 7.9
Triglyceride (mg/dL)	89.9 ± 8.5	90.0 ± 2.6	87.1 ± 5.5	87.2 ± 2.2
Total cholesterol (mg/dL)	89.1 ± 2.3	90.1 ± 1.4	91.0 ± 2.6	92.3 ± 2.4
Alanine aminotransferase (U/L)	20.2 ± 2.0	22.7 ± 1.6	19.8 ± 2.5	18.4 ± 0.9
Aspartate aminotransferase (U/L)	75.7 ± 4.8	72.1 ± 3.0	74.0 ± 3.1	71.0 ± 2.4
Blood urea nitrogen (mg/dL)	0.316 ± 0.005	0.329 ± 0.005	0.325 ± 0.008	0.326 ± 0.002

Data are mean ± SEM.
CON, control group; R20, 20 mg/kg body weight/day red orange complex H extract-administered group; R40, 40 mg/kg body weight/day red orange complex H extract-administered group; R80, 80 mg/kg body weight/day red orange complex H extract-administered group.
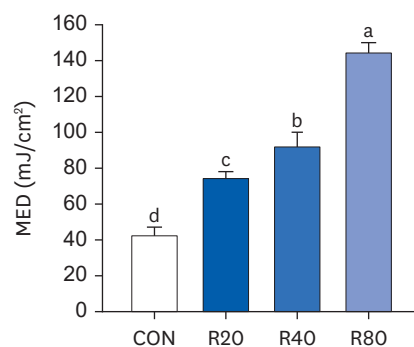
Fig. 1. Effect of ROC administration on the MED of the dorsal skin in Skh:HR-2 mice. ROC was administered via oral gavage for 13 weeks. The backs of mice were divided into 6 sections and irradiated with various UVA-B doses (30, 50, 70, 90, 120, and 150 mJ/cm²). After 24-h UVA-B irradiation, the MED was established. Each bar represents the mean ± SEM (n = 5).
ROC, red orange complex H extract; MED, minimum erythema dose; UV, ultraviolet; CON, control group; R20, 20 mg/kg body weight/day red orange complex H extract-administered group; R40, 40 mg/kg body weight/day red orange complex H extract-administered group; R80, 80 mg/kg body weight/day red orange complex H extract-administered group.
Means without the same letter differ significantly ($P < 0.05$).

ROC ameliorates the photodamage on the dorsal skin of Skh:HR-2 mice

Alterations in 5 skin barrier parameters (erythema, melanin, TEWL, elasticity, and wrinkle index) were evaluated in vehicle- or ROC-administrated mice for 13 weeks to determine whether ROC treatment inhibits the photoaging caused by UV irradiation. The skin erythema index in the UV + C group (144.46 ± 5.4 arbitrary unit [AU]) was significantly higher than that in the NOR group (72.2 ± 6.6 AU). Conversely, the UV + R80 mice (117.3 ± 6.1 AU) showed a significantly lower erythema index (**Fig. 2A**). Next, the UV + C group (205.7 ± 10.0 AU) also had a significantly higher skin melanin index than the NOR group (51.4 ± 8.1 AU). However, the ROC treatment strongly suppressed the melanin production in the UV + R40 (166.3 ± 7.9 AU) and UV + R80 groups (162.1 ± 9.1 AU) (**Fig. 2B**). Further, skin TEWL was measured to assess the skin barrier function. The TEWL of the UV + C group was remarkably higher (15.83 ± 1.51 g/h/m^2) than that of the NOR group (8.43 ± 0.49 g/h/m^2). However, the pretreatment with ROC reduced TEWL. The UV + R40 (11.02 ± 0.33 g/h/m^2, $P < 0.01$) and UV + R80 groups (12.16 ± 0.62 g/h/m^2, $P < 0.05$) were more effective than the UV + R20 group (13.07 ± 1.05 g/h/m^2) (**Fig. 2C**).
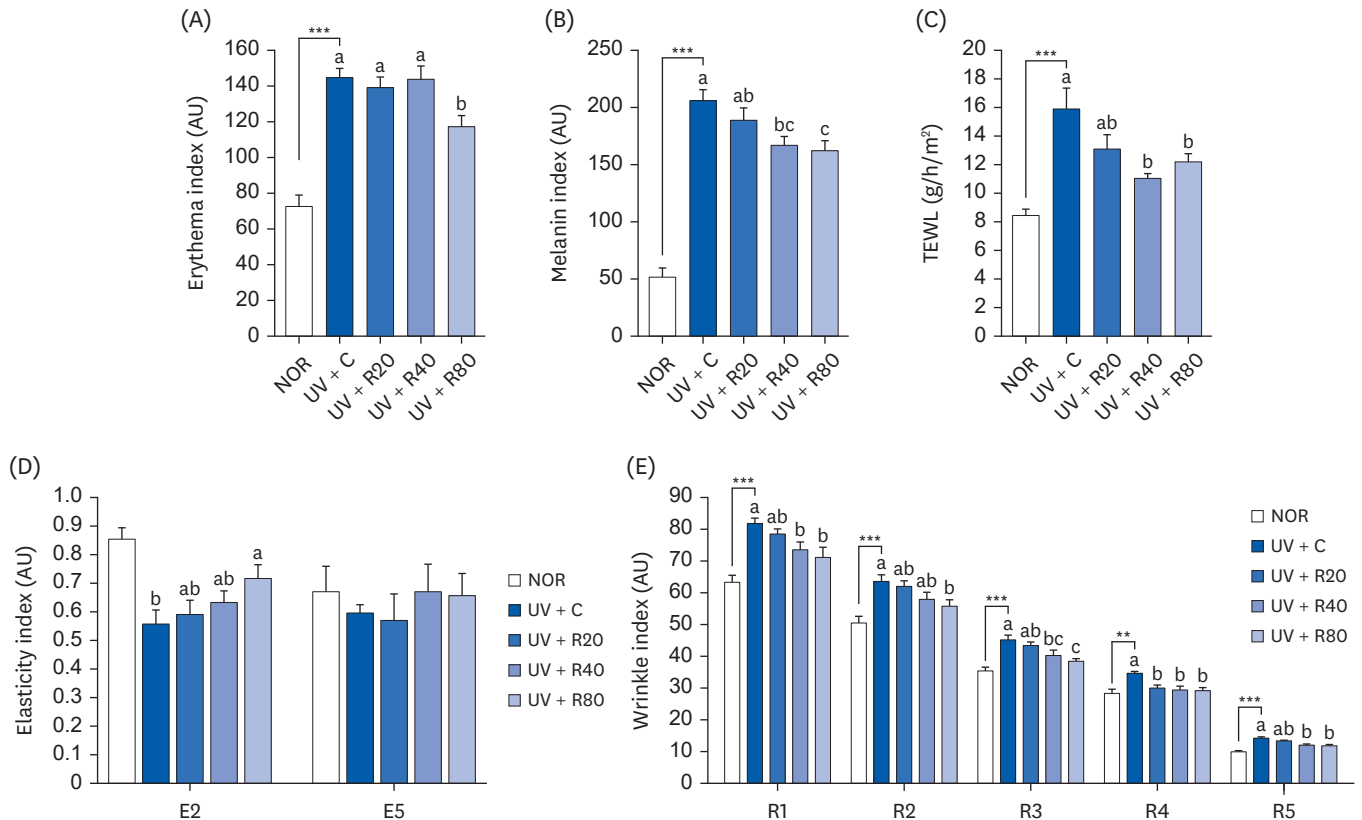
Fig. 2. Effect of ROC administration on skin index in UVA-B-irradiated Skh:HR-2 mice. ROC was administered via oral gavage for 13 weeks. After 3-week ROC administration, mice were exposed to UVA-B irradiation 3 times per week for 10 weeks. Various skin indices were estimated using an individual skin analyzer. (A) Erythema index; (B) Melanin index; (C) TEWL; (D) Elasticity index (E2, gross elasticity; E5, net elasticity); and (E) Wrinkle index (R1, total roughness; R2, average roughness; R3, maximum roughness; R4, smoothness depth; R5, arithmetic average roughness). Each bar represents the mean ± SEM (n = 10).
ROC, red orange complex H extract; UV, ultraviolet; NOR, normal control group; UV + C, ultraviolet-irradiated control group; UV + R20, ultraviolet-irradiated and 20 mg/kg body weight/day red orange complex H extract administration group; UV + R40, ultraviolet-irradiated and 40 mg/kg body weight/day red orange complex H extract administration group; UV + R80, ultraviolet-irradiated and 80 mg/kg body weight/day red orange complex H extract administration group; TEWL, transepidermal water loss; AU, arbitrary unit.
$^{**}P < 0.01$ and $^{***}P < 0.001$ indicate statistically significant differences from the NOR group.
Different letters indicate significant differences among the UV + C, UV + R20, UV + R40, and UV + R80 groups ($P < 0.05$).

The results showed that the skin elasticity (E2, gross elasticity, and E5, net elasticity) of the UV group was lower than that of the NOR group. A significant increase in the skin elasticity (E2) was observed in the 80 mg ROC group (**Fig. 2D**). The E2 values markedly improved by 28% after 13 weeks of treatment. However, the difference in the net elasticity was not statistically significant as compared to that observed in the UV group. Next, we measured the effects of ROC on UV-induced wrinkle formation in hairless mice (**Fig. 2E**). The values indicating skin roughness (R1) in the UV + C group increased significantly by 81.7 ± 1.9 AU. The R1 values in the UV + R40 and UV + R80 groups decreased significantly by 73.2 ± 2.9 AU and 71.1 ± 3.3 AU, respectively. The maximum roughness (R2) was 50.5 ± 2.1 AU and 63.5 ± 2.0 ($P < 0.05$) in the NOR and UV + C groups, respectively. The UV + R80 group displayed significantly lower R2 values (55.7 ± 2.2 AU). The values of the maximum roughness (R3) in the NOR and UV + C groups were 35.2 ± 1.3 AU and 45.0 ± 1.6 AU, respectively. The R3 values in the UV + R80 group were 38.1 ± 1.1 AU. After 13 weeks of treatment, the R1, R2, and R3 values in the UV + R80 group were statistically significantly lower than those in the UV + C group. The smoothness depth (R4) reflects skin roughness. The R4 values in the UV + C group (34.3 ± 0.9 AU) were significantly higher than the ones in the NOR group (28.1 ± 1.5 AU). R4 values were improved in the UV + R20, UV + R40, and UV + R80 groups (29.8 ± 1.0 AU, 29.3 ± 1.4 AU, and 29.1 ± 1.1 AU, respectively). ROC ameliorated the arithmetic average roughness values (R5), which indicated the depth of a shallow wrinkle. R5 values in the UV + C group (14.1 ± 0.5 AU) were higher than those observed in the NOR group (9.8 ± 0.5 AU). R5 values decreased in a statistically significant manner in the UV + R40 and UV + R80 groups (11.8 ± 0.6 AU and 11.6 ± 0.6 AU, respectively). The had improved skin roughness and wrinkle depth were observed in the ROC treatment group compared to those in the UV + C group.

ROC inhibits the release of pro-inflammatory cytokines in hairless mice

Previous studies have reported that UV irradiation induces the production of various inflammatory cytokines such as IL-6 and TNF-α [22]. To determine the effect of ROC on pro-inflammatory cytokine levels, Skh:HR-2 mice were exposed to UV irradiation 3 times per week for ten weeks. Thereafter, the levels of inflammation-associated cytokines IL-6 and TNF-α were measured. As can be seen in **Fig. 3**, the IL-6 and TNF-α protein levels in the UV + C group than were higher than those in the NOR group. However, ROC treatment inhibited this increase. This result suggests that ROC effectively reduces the pro-inflammatory response to UVR.

ROC inhibits skin pigmentation in the dorsal skin in UV-irradiated Skh:HR-2 mice

The inhibitory effects of ROC on skin pigmentation were also examined in hairless mice. Mice were administered with ROC (20, 40, and 80 mg/kg) for 13 weeks along with UV exposure. To determine the effect of ROC on skin pigmentation, Skh:HR-2 mice were exposed to UV irradiation. The melanin content in the skin tissue was then stained with Fontana-Masson's silver. As visible in **Fig. 4A**, the melanin content in the skin of UV-irradiated mice was increased. However, the administration of ROC on UV-irradiated skin reduced the levels of melanin granules as compared with those in the skin of the mice in the UV + C group. In addition, the ROC treatment led to a significantly lower melanin content than that in the NOR group (**Fig. 4B**). These results suggest that ROC affects UV-induced skin pigmentation in mice, particularly through the inhibition of melanogenesis.
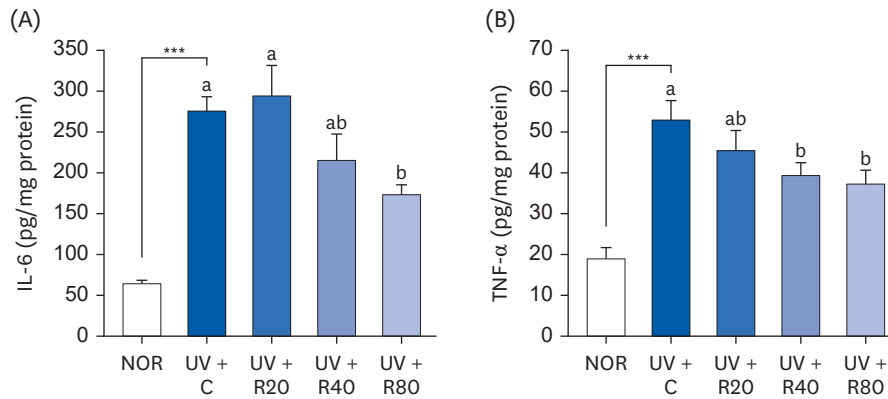
Fig. 3. Effect of ROC administration on IL-6 and TNF-α levels in the dorsal skin in UVA-B-irradiated Skh:HR-2 mice. ROC was administered via oral gavage for 13 weeks. After 3-week ROC administration, mice were exposed to UVA-B irradiation 3 times per week for ten weeks. Dorsal skin tissues were excised and homogenized. The levels of IL-6 (A) and TNF-α (B) in the skin homogenate were measured using enzyme-linked immunosorbent assay kits. Each bar represents the mean ± SEM (n = 10).
ROC, red orange complex H extract; UV, ultraviolet; NOR, normal control group; UV + C, ultraviolet-irradiated control group; UV + R20, ultraviolet-irradiated and 20 mg/kg body weight/day red orange complex H extract administration group; UV + R40, ultraviolet-irradiated and 40 mg/kg body weight/day red orange complex H extract administration group; UV + R80, ultraviolet-irradiated and 80 mg/kg body weight/day red orange complex H extract administration group; IL-6, interleukin-6; TNF-α, tumor necrosis factor-α.
[***]$P < 0.001$ significantly different from the NOR group.
Different letters indicate significant differences among UV + C, UV + R20, UV + R40, and UV + R80 groups ($P < 0.05$).
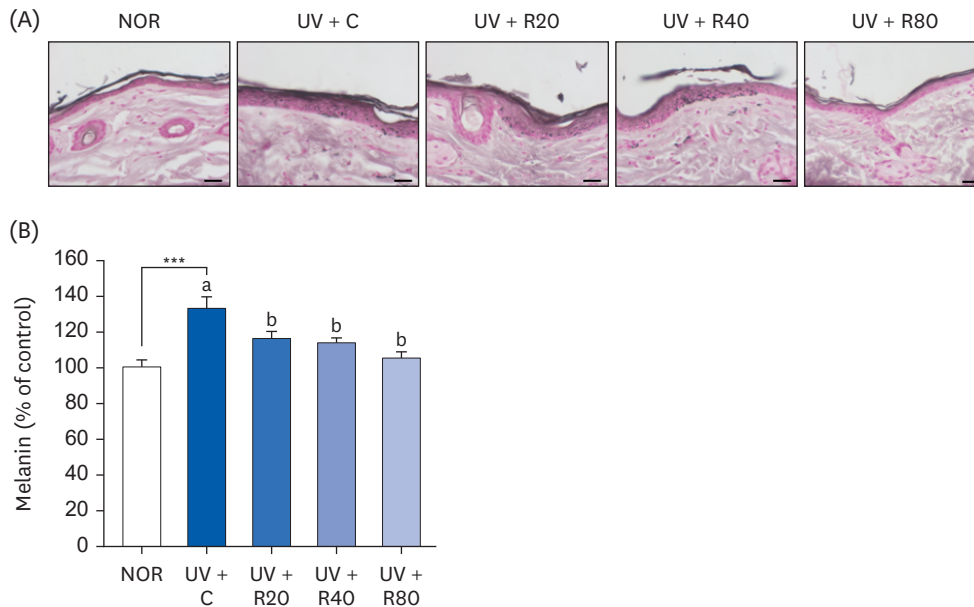
Fig. 4. Effect of ROC administration on melanin content in the dorsal skin in UVA-B-irradiated Skh:HR-2 mice. ROC was administered via oral gavage for 13 weeks. After 3-week ROC administration, mice were exposed to UVA-B irradiation 3 times per week for ten weeks. (A) Dorsal skin sections were stained with Fontana-Masson's silver stain. Representative images of staining are presented. Scale bar, 50 μm. (B) Melanin content in the dorsal skin. Each bar represents the mean ± SEM (n = 10).
ROC, red orange complex H extract; UV, ultraviolet; NOR, normal control group; UV + C, ultraviolet-irradiated control group; UV + R20, ultraviolet-irradiated and 20 mg/kg body weight/day red orange complex H extract administration group; UV + R40, ultraviolet-irradiated and 40 mg/kg body weight/day red orange complex H extract administration group; UV + R80, ultraviolet-irradiated and 80 mg/kg body weight/day red orange complex H extract administration group.
[***]$P < 0.001$ indicates statistically significant differences from the NOR group.
Different letters indicate significant differences among UV + C, UV + R20, UV + R40, and UV + R80 groups ($P < 0.05$).

ROC enhances HA in UV-irradiated Skh:HR-2 mice

HA is a valuable skin component of cutaneous ECM and is used for measuring the skin-moisturizing capacity. This study examined the regulation of HA metabolism following ROC administration. Our results showed that the HA content in the UV + C group (41.1 ± 3.5 µg/mg protein) differed from that in the NOR group (66.5 ± 4.2 µg/mg protein; $P < 0.05$; **Fig. 5A**). The UV-induced reduction in HA production in the skin tissues was inhibited by ROC administration. Compared with the UV + C group, the HA levels in the UV + R20 group mice were decreased by 47.4%, whereas those in the mice in the UV + R40 and UV + R80 groups were increased by 55.7%. Therefore, the HA rescue was enhanced by the co-administration of ROC and UV irradiation. HAS and aquaporin 3 (AQP3), expressed in human fibroblasts and keratinocytes, are well-known moisturizing factors. The mRNA expression of HA synthesizing (*Has1*, *Has2*, and *Has3*) and *Aqp3* genes in the UV-irradiated hairless mice tissues was also significantly increased by the ROC treatment in a dose-dependent manner in the respective different-UV dose-treated groups (**Fig. 5B and D**). To clarify the specific mechanism of HA degradation, the gene expression of hyaluronidase 1 (*Hyal1*) in skin tissues was further analyzed. A decrease in the *Hyal1* mRNA expression levels was observed in the UV + R40 group (**Fig. 5C**). We found that ROC both
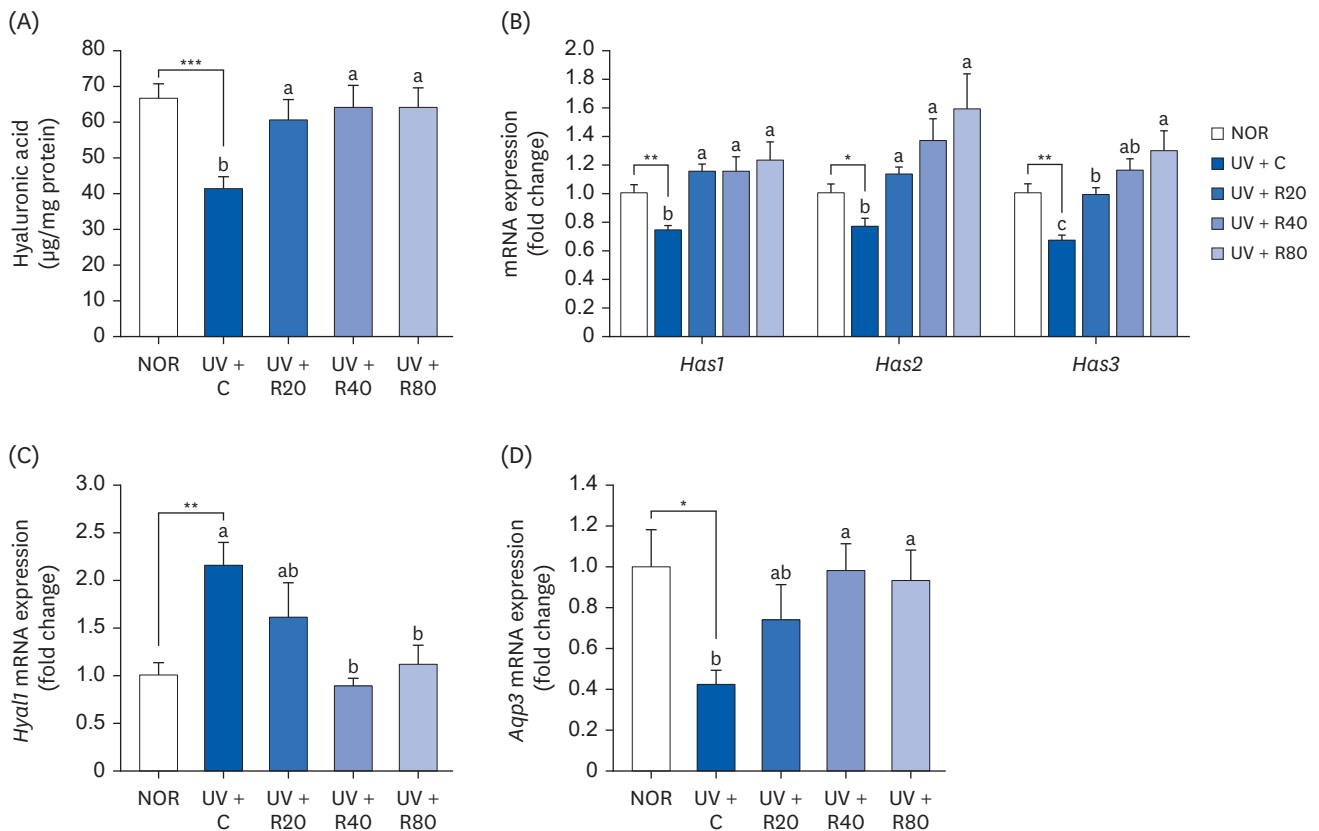
Fig. 5. Effect of ROC administration on HA synthesis in the dorsal skin in UVA-B-irradiated Skh:HR-2 mice. ROC was administered via oral gavage for 13 weeks. After 3-week ROC administration, mice were exposed to UVA-B irradiation 3 times per week for 10 weeks. (A) Dorsal skin tissues were excised and homogenized. HA levels in the skin homogenate were measured using enzyme-linked immunosorbent assay kits. (B-D) Total RNA in the dorsal skin tissues was extracted and reverse-transcribed, and real-time polymerase chain reaction was conducted. The expression of each mRNA was normalized to that of *Gapdh* and is represented relative to that of the NOR group. Each bar represents the mean ± SEM (n = 10).
ROC, red orange complex H extract; HA, hyaluronic acid; UV, ultraviolet; NOR, normal control group; UV + C, UV-irradiated control group; UV + R20, UV-irradiated and 20 mg/kg body weight/day red orange complex H extract administration group; UV + R40, UV-irradiated and 40 mg/kg body weight/day red orange complex H extract administration group; UV + R80, UV-irradiated and 80 mg/kg body weight/day red orange complex H extract administration group; *Has*, hyaluronic acid synthase; *Hyal*, hyaluronidase; *Aqp3*, aquaporin 3; *Gapdh*, glyceraldehyde 3-phosphate dehydrogenase.
*$P < 0.05$, **$P < 0.01$, and ***$P < 0.001$ indicate statistically significant differences from the NOR group.
Different letters indicate significant differences among UV + C, UV + R20, UV + R40, and UV + R80 groups ($P < 0.05$).

promoted HA production in the skin tissues and decreased HA degradation. Therefore, ROC may effectively prevent UV-induced reduction in the HA levels in hairless mice.

ROC increases the collagen production in UV-irradiated Skh:HR-2 mice

The effect of ROC administration on collagen content was investigated in UV-exposed skin of hairless mice. The collagen production (in relative fluorescence units) in the skin of the UV-irradiated mice was significantly lower than that in the NOR group mice. However, the collagen production values in the UV + R40 and UV + R80 groups were significantly higher than those in the NOR group (**Fig. 6A and B**). In this study, we investigated the effect of 13-week co-administration of ROC and UV irradiation on the expression of collagen type 1 alpha 1 chain (*Col1a1*), *Col3a1*, *Col4a1*, and *Col7a1* mRNA, which is associated with collagen synthesis. As can be observed in **Fig. 6C**, the gene expression of collagen types 3 and 4 was strongly elevated in the UV + ROC-treated groups. These results suggest that the oral administration of ROC increased the skin collagen content and mRNA expression of genes related to collagen synthesis in our UV-induced photoaging *in vivo* model.

ROC suppresses MMP expression in UV-irradiated Skh:HR-2 mice

UV irradiation promotes the expression of MMPs, which play leading roles in ECM degradation and activation of the MAPK signaling pathway during skin aging [23,24]. To
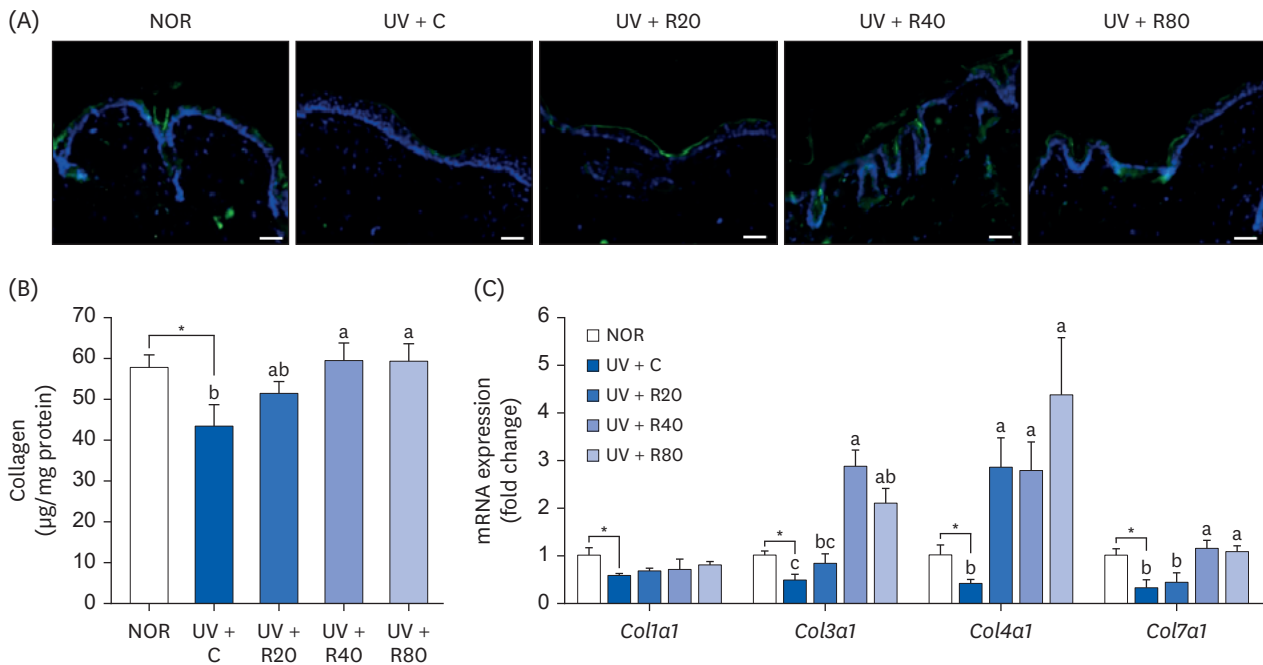
Fig. 6. Effect of ROC administration on collagen synthesis in the dorsal skin in UVA-B-irradiated Skh:HR-2 mice. ROC was administered via oral gavage for 13 weeks. After 3-week ROC administration, mice were exposed to UVA-B irradiation 3 times per week for ten weeks. (A) Dorsal skin sections were stained with collagen 1 antibody. Representative immunofluorescence staining images are displayed. Scale bar, 50 μm. (B) Dorsal skin tissues were excised and homogenized. The levels of collagen in skin homogenates were measured using hyaluronic acid enzyme-linked immunosorbent assay kits. (C) Total RNA in the dorsal skin tissues was extracted, reverse-transcribed, and subjected to real-time polymerase chain reaction. The expression of each mRNA was normalized to that of *Gapdh* and is represented relative to that of the NOR group. Each bar represents the mean ± SEM (n = 10).
ROC, red orange complex H extract; UV, ultraviolet; NOR, normal control group; UV + C, ultraviolet-irradiated control group; UV + R20, ultraviolet-irradiated and 20 mg/kg body weight/day red orange complex H extract administration group; UV + R40, ultraviolet-irradiated and 40 mg/kg body weight/day red orange complex H extract administration group; UV + R80, ultraviolet-irradiated and 80 mg/kg body weight/day red orange complex H extract administration group; *Col1a1*, collagen type 1 alpha 1 chain; *Col3a1*, collagen type 3 alpha 1 chain; *Col4a1*, collagen type 4 alpha 1 chain; *Col7a1*, collagen type 7 alpha 1 chain; *Gapdh*, glyceraldehyde 3-phosphate dehydrogenase.
*$P < 0.05$, significantly different from the NOR group.
Different letters indicate significant differences among UV + C, UV + R20, UV + R40, and UV + R80 groups ($P < 0.05$).

investigate whether ROC influenced the expression of gelatinase and collagenase, mice were treated with various concentrations of ROC after UV irradiation. We established the effects of the oral administration of ROC on MAPK activation and downstream MMP-2 and MMP-13 proteins in UV-irradiated Skh:HR-2 mice skin. UV irradiation significantly increased MMP-2 and MMP-13 protein expression, whereas the induction was markedly suppressed in the ROC-treated group as compared to the UV + C group (**Fig. 7A and B**). Moreover, *Mmp-2* and *Mmp-13* mRNA levels showed a trend toward a significant decrease in the UV + R20, UV + R40, and UV + R80 groups as compared to that in the UV + C group (**Fig. 7C**).

ROC suppresses UV-induced phosphorylation of JNK and AP-1 activation in UV-irradiated Skh:HR-2 mice

We examined whether ROC could suppress the UV-induced phosphorylation of MAPK, including JNK and AP-1. As can be seen in **Fig. 8A and B**, UV irradiation increased JNK phosphorylation. ROC treatment inhibited JNK phosphorylation in the UV-treated mice in the UV-R20 and UV + R80 groups, whereas the phosphorylation of JNK in the UV + R40 group was not significantly affected by the ROC treatment. These results suggest that orally administered ROC suppresses MMP and inhibits activated JNK protein expression in UV-irradiated skin tissues by regulating the MAPK signaling pathway.
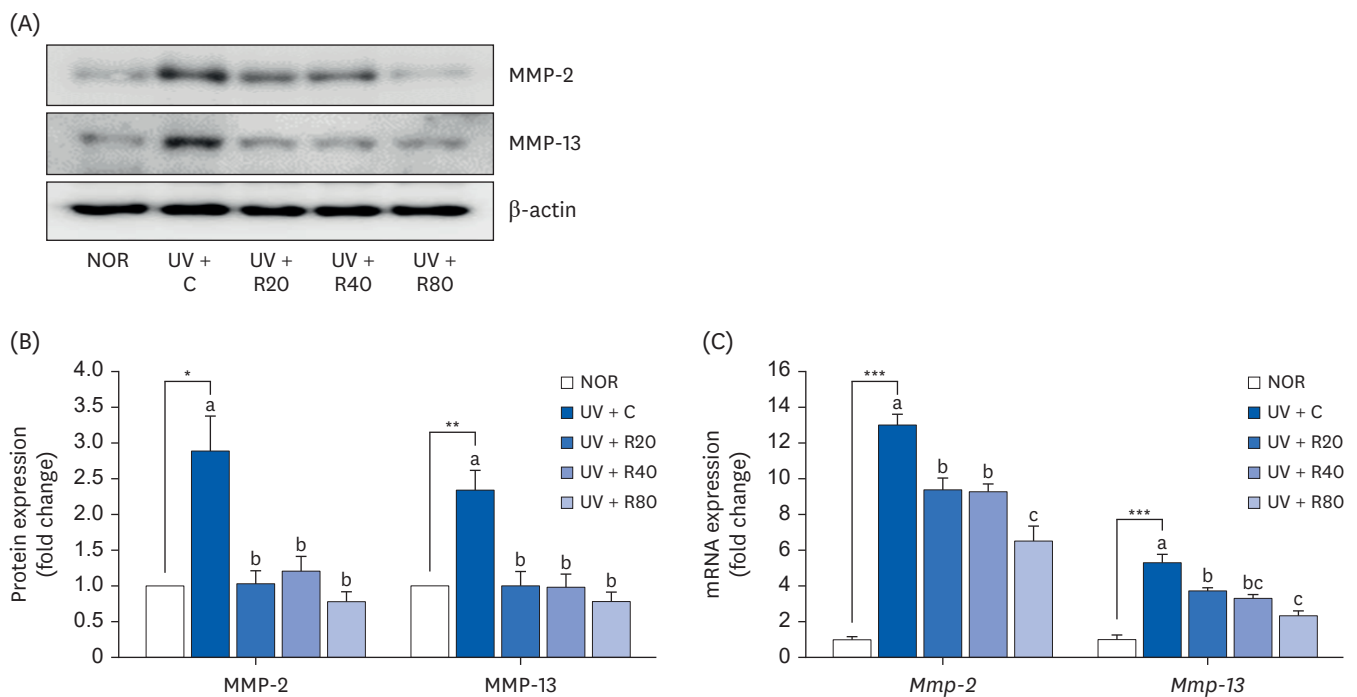
Fig. 7. Effect of ROC administration on MMP-2 and MMP-13 expression in the dorsal skin in UVA-B-irradiated Skh:HR-2 mice. ROC was administered via oral gavage for 13 weeks. After 3-week ROC administration, mice were exposed to UVA-B irradiation 3 times per week for ten weeks. (A) Total lysates of dorsal skin tissues were prepared and analyzed using Western blotting with the indicated antibodies. Images of Western blots representative of 3 independent experiments are displayed. (B) Quantitative analysis of Western blot results. The protein abundance was normalized to β-actin and expressed relative to that of the NOR group. (C) Total RNA in the dorsal skin tissues was extracted, reverse-transcribed, and subjected to real-time polymerase chain reaction. The expression of each mRNA was normalized to that of *Gapdh* and is represented relative to that of the NOR group. Each bar represents the mean ± SEM (n = 10).
ROC, red orange complex H extract; UV, ultraviolet; NOR, normal control group; UV + C, ultraviolet-irradiated control group; UV + R20, ultraviolet-irradiated and 20 mg/kg body weight/day ROC administration group; UV + R40, ultraviolet-irradiated and 40 mg/kg body weight/day ROC administration group; UV + R80, ultraviolet-irradiated and 80 mg/kg body weight/day ROC administration group; MMP, matrix metallopeptidase; *Gapdh*, glyceraldehyde 3-phosphate dehydrogenase.
$^{*}P < 0.05$, $^{**}P < 0.01$, $^{***}P < 0.001$ significantly different from the NOR group.
Different letters indicate significant differences among UV + C, UV + R20, UV + R40, and UV + R80 groups ($P < 0.05$).

(A)

(B)

(C)
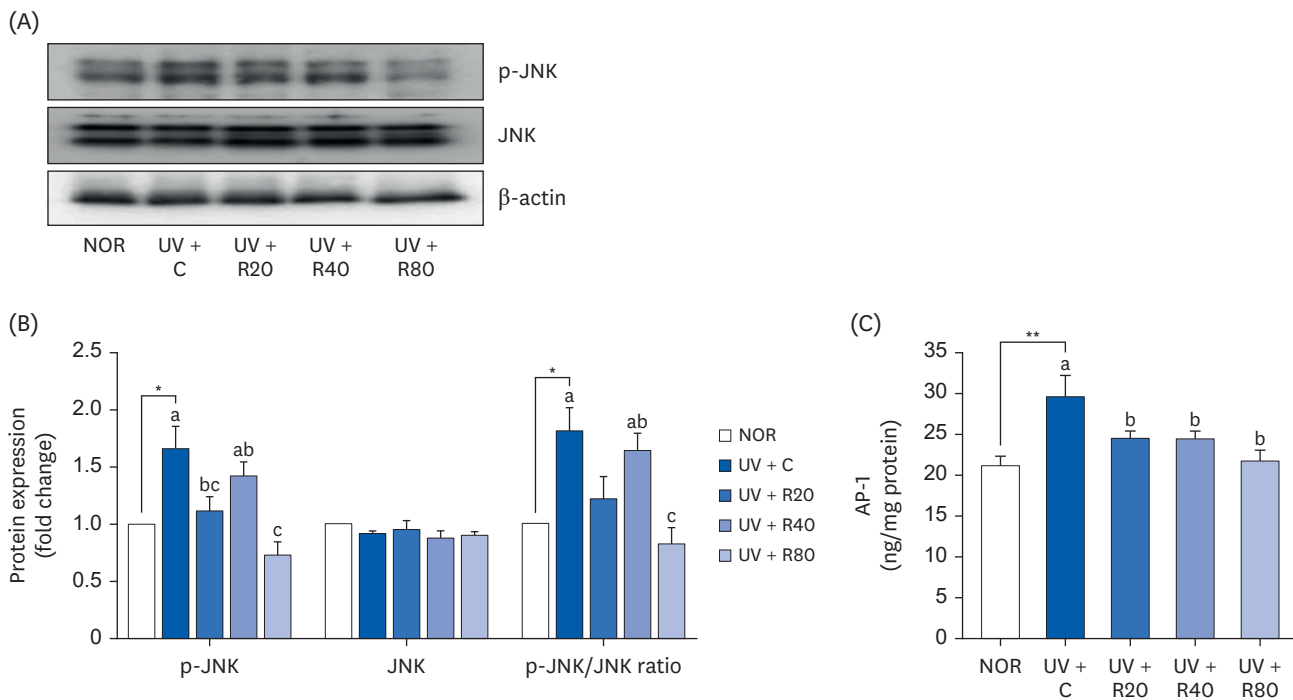
Fig. 8. Effect of ROC administration on JNK signaling pathway in the dorsal skin in UVA-B-irradiated Skh:HR-2 mice. ROC was administered via oral gavage for 13 weeks. After 3-week ROC administration, mice were exposed to UVA-B irradiation 3 times per week for ten weeks. (A) Total lysates of dorsal skin tissues were prepared and analyzed using Western blotting with the indicated antibodies. Images of Western blots representative of 3 independent experiments are displayed. (B) Quantitative analysis of Western blot results. The protein abundance was normalized to β-actin and expressed relative to that of the NOR group. (C) Nuclear protein from dorsal skin tissues was extracted, and the AP-1 content in the nuclear protein was measured. Each bar represents the mean ± SEM (n = 10).
ROC, red orange complex H extract; UV, ultraviolet; NOR, normal control group; UV + C, ultraviolet-irradiated control group; UV + R20, ultraviolet-irradiated and 20 mg/kg body weight/day red orange complex H extract administration group; UV + R40, ultraviolet-irradiated and 40 mg/kg body weight/day red orange complex H extract administration group; UV + R80, ultraviolet-irradiated and 80 mg/kg body weight/day red orange complex H extract administration group; p-JNK, phospho c-Jun NH2-terminal kinase; JNK, c-Jun NH2-terminal kinase; AP-1, activator protein 1.
*$P < 0.05$, **$P < 0.01$ statistically significant differences from the NOR group.
Different letters indicate significant differences among UV + C, UV + R20, UV + R40, and UV + R80 groups ($P < 0.05$).

JNK activation is crucial for c-Jun, which is involved in AP-1 activation in combination with c-Fos. AP-1 is a transcription factor that plays an important role in the regulation of MMP-2 and MMP-13 expression. To investigate AP-1 activity in mouse skin tissues, the nuclear protein was separated from the skin tissues, and the AP-1 content was measured. AP-1 expression was suppressed in a dose-dependent manner by the ROC treatment (**Fig. 8C**). AP-1 was higher in the UV + C group (29.68 ± 2.60 ng/mg protein) than in the NOR group (21.12 ± 1.27 ng/mg protein). ROC administration decreased the AP-1 levels in the UV + R20, UV+40, and UV + R80 groups (24.286 ± 0.98 ng/mg protein, 24.431 ± 1.01 ng/mg protein, and 21.685 ± 1.39 ng/mg protein, respectively).

DISCUSSION

Photoaging is caused by prolonged exposure to UVR and elicits adverse histological and clinical damage to the skin, such as skin thickening, deeper wrinkle formation, rough and dry skin texture, hyperpigmentation, inflammation, and cancer [25,26]. In recent years, numerous studies have evidenced that a large number of natural constituent-derived dietary supplements possess photoprotective efficacy against UV irradiation owing to their large amounts of phytochemicals [27,28].

For this reason, several reported beneficial effects of ROC have attracted scientific attention, such as its anti-inflammatory properties, anti-oxidant activity, and cardiovascular protection [12,16,29-33]. In this study, we evaluated the effects of 13-week oral ROC administration on UV-irradiated skin damage in Skh:HR-2 mice. We investigated the changes in skin parameters (erythema, melanin, TEWL, elasticity, and wrinkles), inflammatory cytokines (IL-6 and TNF-α), and skin composition (melanin, HA, and collagen) in response to ROC administration. The continuous exposure to UV irradiation reduced skin moisture and elasticity, resulting in dry and rough skin [34,35]. TEWL, which represents the amount of water loss, is inversely proportional to skin hydration and shows damage to skin barrier function. Herein, ROC administration significantly reduced the TEWL of the skin relative to that of the UV-irradiated group (**Fig. 2C**, $P < 0.05$), whereas skin hydration was higher than that in the UV-irradiated group (**Fig. 5**). Corresponding to this enhancement in skin moisturizing, the highest dose group (UV + R80) showed a statistically significant decrease in erythema, melanin index and wrinkle index, and increased elasticity index compared with the UV-treated group. These data support the notion that the recovery effect of daily ROC administration alleviates UV-induced skin barrier damage in the skin of hairless mice.

Skin hydration is essential for the normal functioning of the outer skin layer [36]. HA, one of the most abundant components of the epidermis, is crucial for maintaining moisture levels. UV irradiation disrupts HA turnover in the dermis, as well as the metabolism of 3 different isoforms of HAS1–3, water- and glycerol-transporting protein (AQP3), and hyaluronic acid-degrading enzyme HYAL1 [37]. Notably, the results of the current study showed that the normal levels of the mRNA expression, associated with skin moisturizing and barrier function (*Has1*, *Has2*, *Has3*, and *Aqp3*), were recovered to after ROC administration (**Fig. 5**). However, ROC decreased the expression level of *Hyal1*, which was lower than that of the UV + C group. Yun *et al*. [38] reported that *Agastache rugosa* extract possesses a skin hydration ability, as evidenced by improving TEWL, HA levels via upregulating HAS gene expression. In addition, Razia *et al*. [39] established that *Aloe vera* flower water extract increased AQP3 expression and HA synthesis via regulation of HAS1 and HYAL1 protein. Supplementing photoaged mice with ROC markedly increased HA content and enhanced skin hydration by increasing the expression of HASs and decreasing HA degradation, consequently contributing to enhanced TEWL levels in the skin tissues. All these results reveal the defensive skin hydration effects mediated by ROC against UV-induced conditions.

Collagen is the most common fiber-forming protein and is the main structural element in the ECM. Collagen types I and III, encoded by *COL1A1* and *COL3A1* genes, respectively, are the major types of fibrillar collagen produced by fibroblasts. The *COL4A1* gene encodes a type IV collagen, alpha IV collagen, a flexible protein important for the structural integrity of many tissues and an integral component of basement membranes. *COL7A1* encodes a protein called the pro-α1(VII) chain. In this study, ROC markedly elevated the mRNA expression levels of the collagen synthesis genes *Col3a1*, *Col4a1*, and *Col7a1* in the UV-induced conditions. Specifically, at a dose of 80 mg/kg, ROC increased the type-IV procollagen content by 56%. UV irradiation activated MAPK/AP-1 signaling. The stimulation of MAPK, consisting of c-Jun and c-Fos, upregulates AP-1 activity, which improves MMP expression. MMPs are a large group of zinc-dependent endopeptidases that are responsible for ECM remodeling, including collagen fiber and elastin degradation by UV exposed skin tissues, and thus contribute to wrinkle formation and the phenotype of photoaged human skin. AP-1 regulates several MMPs, which are classified according to their substrate preference as follows: collagenases (MMP-1, MMP-8, and MMP-13), gelatinases (MMP-2 and MMP-9), and stromelysins (MMP-3,

MMP-10, and MMP-11). Pretreatment with ROC significantly reduced the UV-B-stimulated MMP-1 and MMP-9 mRNA expression/protein and type I collagen translation levels in human skin fibroblasts [16]. Hesperidin, a flavanone glycoside, which is abundant in ROC, reportedly downregulates MMP-9 expression. Hesperidin reduced the expression of pro-inflammatory cytokines and decreased the TEWL, skin thickness, wrinkle formation, and collagen fiber loss in UV-induced photoaging in hairless skin tissue [40]. In the present animal model experiment, ROC remarkably decreased the protein and mRNA expression of MMP-2, a type IV collagenase, and MMP-13, a collagenase 3 (**Fig. 7**). The effect of UV irradiation on MMP expression differed between *in vitro* and *in vivo* models, but the harmful effect of UV exposure on the skin was suppressed by ROC administration. ROC also downregulated the protein levels of p-JNK and significantly reduced those of AP-1 components as compared to the ones of the UV group (**Fig. 8**). These results are in agreement with those of a study carried out by Park *et al.* [41] who found that the ethanol extract of *Kaempferia parviflora* increased collagen type I, III, and VII, and induced a significant reduction in MMPs via the suppression of c-JNK and c-Fos activity in UVB-induced mice. Another study was performed by Han *et al.* [42] in which the oral administration of *Hydrangea serrata* leaves extract significantly increased the pro-COL1A1 and HA production, but decreased the level of MMPs and inflammatory cytokines through AP-1 and the MAPK signaling pathway in UVB-exposed mice. These results suggest that ROC alleviates the protein and mRNA expression of MMPs by deactivating the MAPK/AP-1 pathway, with a concurrent reduction in collagen degradation.

UV exposure induces the secretion of various pro-inflammatory cytokines, such as TNF-α, IL-1β, IL-6, IL-8, and IL-10, from keratinocytes, which results in erythema, edema, and influx of inflammatory cells into the epidermal keratinocytes and dermal fibroblasts. These cytokines upregulate MMP expression, which not only degrades elastic fibers but also leads to the formation of wrinkles. In this study, UV irradiation increased IL-6 and TNF-α levels. It was previously reported that ROC significantly downregulated pro-inflammatory cytokines, such as IL-6 and TNF-α, compared with the UVB-irradiated human cell lines [16]. Previous and the present results confirm that the anti-photoaging effects of ROC are related to its anti-inflammatory activities. **Fig. 9** illustrates the proposed mechanism through which ROC improves UV-induced photoaging in hairless mice.

In conclusions, the anti-photoaging effects of ROC were investigated in UV-irradiated Skh:HR-2 mice treated with ROC (20, 40, and 80 mg/kg/day). ROC recovered the skin parameters (erythema, melanin, TEWL, elasticity, and wrinkle indices) compared with UV-irradiated mice. ROC treatment increased the mRNA levels of HA synthesis genes (*Has1*, *Has2*, and *Has3*), while suppressing the MMP-2 and MMP-13 expression and increasing the expression of collagen synthases. ROC has strong anti-inflammatory properties exerted through its suppressive activities against IL-6 and TNF-α secretion and accumulation and melanin synthesis downregulation. Collectively, our data evidenced that ROC attenuates UV-induced photoaging in hairless mice and can thus serve as a natural anti-photoaging nutraceutical.
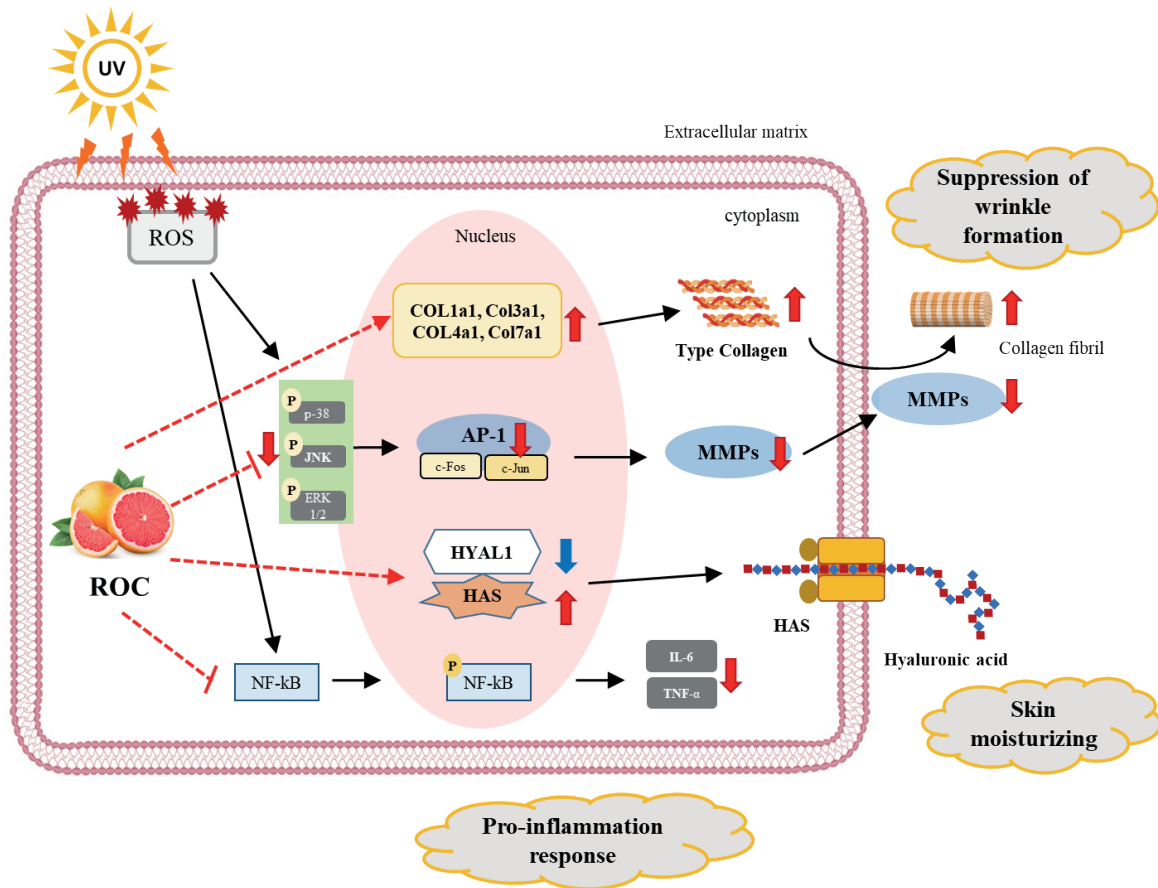
Fig. 9. Summary of the effects of the ROC on the photoaging.
UV, ultraviolet; ROS, reactive oxygen species; ROC, red orange complex H extract; JNK, c-Jun NH2-terminal kinase; ERK1/2, extracellular signal-regulated kinase 1/2; AP-1, activator protein 1; MMP, matrix metalloproteinases; COL1a1, collagen type 1 alpha 1 chain; COL3a1, collagen type 3 alpha 1 chain; COL4a1, collagen type 4 alpha 1 chain; COL7a1, collagen type 7 alpha 1 chain; HYAL1, hyaluronidase 1; HAS, hyaluronic acid synthase; NF-κB, nuclear factor-κB; IL-6, interleukin 6; TNF-α, tumor necrosis factor α.

ACKNOWLEDGMENTS

SUPPLEMENTARY MATERIAL

Supplementary Table 1
Primer sequences used in this study

Click here to view

REFERENCES

1. Parrado C, Mercado-Saenz S, Perez-Davo A, Gilaberte Y, Gonzalez S, Juarranz A. Environmental stressors on skin aging. Mechanistic insights. Front Pharmacol 2019;10:759.
   PUBMED | CROSSREF

2. Gilchrest BA, Yaar M. Ageing and photoageing of the skin: observations at the cellular and molecular level. Br J Dermatol 1992;127 Suppl 41:25-30.
   PUBMED | CROSSREF

3. Cavinato M, Waltenberger B, Baraldo G, Grade CVC, Stuppner H, Jansen-Dürr P. Plant extracts and natural compounds used against UVB-induced photoaging. Biogerontology 2017;18:499-516.
   PUBMED | CROSSREF

4. Chiang HM, Chen HC, Lin TJ, Shih IC, Wen KC. *Michelia alba* extract attenuates UVB-induced expression of matrix metalloproteinases via MAP kinase pathway in human dermal fibroblasts. Food Chem Toxicol 2012;50:4260-9.
   PUBMED | CROSSREF

5. Hwang E, Park SY, Lee HJ, Lee TY, Sun ZW, Yi TH. Gallic acid regulates skin photoaging in UVB-exposed fibroblast and hairless mice. Phytother Res 2014;28:1778-88.
   PUBMED | CROSSREF

6. Gromkowska-Kępka KJ, Puścion-Jakubik A, Markiewicz-Żukowska R, Socha K. The impact of ultraviolet radiation on skin photoaging - review of *in vitro* studies. J Cosmet Dermatol 2021;20:3427-31.
   PUBMED | CROSSREF

7. Matsumura Y, Ananthaswamy HN. Toxic effects of ultraviolet radiation on the skin. Toxicol Appl Pharmacol 2004;195:298-308.
   PUBMED | CROSSREF

8. Shaulian E, Karin M. AP-1 as a regulator of cell life and death. Nat Cell Biol 2002;4:E131-6.
   PUBMED | CROSSREF

9. Geoffrey K, Mwangi AN, Maru SM. Sunscreen products: rationale for use, formulation development and regulatory considerations. Saudi Pharm J 2019;27:1009-18.
   PUBMED | CROSSREF

10. Parrado C, Philips N, Gilaberte Y, Juarranz A, González S. Oral photoprotection: effective agents and potential candidates. Front Med (Lausanne) 2018;5:188.
    PUBMED | CROSSREF

11. Cimino F, Cristani M, Saija A, Bonina FP, Virgili F. Protective effects of a red orange extract on UVB-induced damage in human keratinocytes. Biofactors 2007;30:129-38.
    PUBMED | CROSSREF

12. Saija A, Tomaino A, Lo Cascio R, Rapisarda P, Dederen JC. *In vitro* antioxidant activity and *in vivo* photoprotective effect of a red orange extract. Int J Cosmet Sci 1998;20:331-42.
    PUBMED | CROSSREF

13. Vitali F, Pennisi C, Tomaino A, Bonina F, De Pasquale A, Saija A, Tita B. Effect of a standardized extract of red orange juice on proliferation of human prostate cells *in vitro*. Fitoterapia 2006;77:151-5.
    PUBMED | CROSSREF

14. Bonina FP, Puglia C, Frasca G, Cimino F, Trombetta D, Tringali G, Roccazzello A, Insiriello E, Rapisarda P, Saija A. Protective effects of a standardised red orange extract on air pollution-induced oxidative damage in traffic police officers. Nat Prod Res 2008;22:1544-51.
    PUBMED | CROSSREF

15. Balestra C, Cimino F, Theunissen S, Snoeck T, Provyn S, Canali R, Bonina A, Virgili F. A red orange extract modulates the vascular response to a recreational dive: a pilot study on the effect of anthocyanins on the physiological consequences of scuba diving. Nat Prod Res 2016;30:2101-6.
    PUBMED | CROSSREF

16. Tomasello B, Malfa GA, Acquaviva R, La Mantia A, Di Giacomo C. Phytocomplex of a standardized extract from red orange (*Citrus sinensis* L. Osbeck) against photoaging. Cells 2022;11:1447.
    PUBMED | CROSSREF

17. Nobile V, Burioli A, Yu S, Zhifeng S, Cestone E, Insolia V, Zaccaria V, Malfa GA. Photoprotective and antiaging effects of a standardized red orange (*Citrus sinensis* (L.) Osbeck) extract in Asian and Caucasian subjects: a randomized, double-blind, controlled study. Nutrients 2022;14:2241.
    PUBMED | CROSSREF

18. Peng LH, Liu S, Xu SY, Chen L, Shan YH, Wei W, Liang WQ, Gao JQ. Inhibitory effects of salidroside and paeonol on tyrosinase activity and melanin synthesis in mouse B16F10 melanoma cells and ultraviolet B-induced pigmentation in guinea pig skin. Phytomedicine 2013;20:1082-7.
    PUBMED | CROSSREF

19. Lee HS, Lim SM, Jung JI, Kim SM, Lee JK, Kim YH, Cha KM, Oh TK, Moon JM, Kim TY, et al. *Gynostemma pentaphyllum* extract ameliorates high-fat diet-induced obesity in C57BL/6N mice by upregulating SIRT1. Nutrients 2019;11:2475.
    PUBMED | CROSSREF

20. Cho HJ, Kim WK, Kim EJ, Jung KC, Park S, Lee HS, Tyner AL, Park JH. Conjugated linoleic acid inhibits cell proliferation and ErbB3 signaling in HT-29 human colon cell line. Am J Physiol Gastrointest Liver Physiol 2003;284:G996-1005.
    PUBMED | CROSSREF

21. US Food and Drug Administration. Guidance for Industry: Estimating the Maximum Safe Starting Dose in Initial Clinical Trials for Therapeutics in Adult Healthy Volunteers. Rockville (MD): US Food and Drug Administration; 2005.

22. Yoshizumi M, Nakamura T, Kato M, Ishioka T, Kozawa K, Wakamatsu K, Kimura H. Release of cytokines/chemokines and cell death in UVB-irradiated human keratinocytes, HaCaT. Cell Biol Int 2008;32:1405-11.
    PUBMED | CROSSREF

23. Duan X, Wu T, Liu T, Yang H, Ding X, Chen Y, Mu Y. Vicenin-2 ameliorates oxidative damage and photoaging via modulation of MAPKs and MMPs signaling in UVB radiation exposed human skin cells. J Photochem Photobiol B 2019;190:76-85.
    PUBMED | CROSSREF

24. Pittayapruek P, Meephansan J, Prapapan O, Komine M, Ohtsuki M. Role of matrix metalloproteinases in photoaging and photocarcinogenesis. Int J Mol Sci 2016;17:868.
    PUBMED | CROSSREF

25. Choi SI, Jung TD, Cho BY, Choi SH, Sim WS, Han X, Lee SJ, Kim YC, Lee OH. Anti-photoaging effect of fermented agricultural by-products on ultraviolet B-irradiated hairless mouse skin. Int J Mol Med 2019;44:559-68.
    PUBMED | CROSSREF

26. Young AR. Acute effects of UVR on human eyes and skin. Prog Biophys Mol Biol 2006;92:80-5.
    PUBMED | CROSSREF

27. Saewan N, Jimtaisong A. Natural products as photoprotection. J Cosmet Dermatol 2015;14:47-63.
    PUBMED | CROSSREF

28. Yadav T, Mishra S, Das S, Aggarwal S, Rani V. Anticedants and natural prevention of environmental toxicants induced accelerated aging of skin. Environ Toxicol Pharmacol 2015;39:384-91.
    PUBMED | CROSSREF

29. Grosso G, Galvano F, Mistretta A, Marventano S, Nolfo F, Calabrese G, Buscemi S, Drago F, Veronesi U, Scuderi A. Red orange: experimental models and epidemiological evidence of its benefits on human health. Oxid Med Cell Longev 2013;2013:157240.
    PUBMED | CROSSREF

30. de Lima LP, de Paula BA. A review of the lipolytic effects and the reduction of abdominal fat from bioactive compounds and Moro orange extracts. Heliyon 2021;7:e07695.
    PUBMED | CROSSREF

31. Ribeiro AP, Pereira AG, Todo MC, Fujimori AS, Dos Santos PP, Dantas D, Fernandes AA, Zanati SG, Hassimotto NM, Zornoff LA, et al. Pera orange (*Citrus sinensis*) and Moro orange (*Citrus sinensis* (L.) Osbeck) juices attenuate left ventricular dysfunction and oxidative stress and improve myocardial energy metabolism in acute doxorubicin-induced cardiotoxicity in rats. Nutrition 2021;91-92:111350.
    PUBMED | CROSSREF

32. Buscemi S, Rosafio G, Arcoleo G, Mattina A, Canino B, Montana M, Verga S, Rini G. Effects of red orange juice intake on endothelial function and inflammatory markers in adult subjects with increased cardiovascular risk. Am J Clin Nutr 2012;95:1089-95.
    PUBMED | CROSSREF

33. Magalhães ML, de Sousa RV, Miranda JR, Konig IF, Wouters F, Souza FR, Simão SD, da Silva LA, Nelson DL, das Graças CM. Effects of Moro orange juice (*Citrus sinensis* (L.) Osbeck) on some metabolic and morphological parameters in obese and diabetic rats. J Sci Food Agric 2021;101:1053-64.
    PUBMED | CROSSREF

34. Jiang SJ, Chu AW, Lu ZF, Pan MH, Che DF, Zhou XJ. Ultraviolet B-induced alterations of the skin barrier and epidermal calcium gradient. Exp Dermatol 2007;16:985-92.
    PUBMED | CROSSREF

35. Haratake A, Uchida Y, Schmuth M, Tanno O, Yasuda R, Epstein JH, Elias PM, Holleran WM. UVB-induced alterations in permeability barrier function: roles for epidermal hyperproliferation and thymocyte-mediated response. J Invest Dermatol 1997;108:769-75.
    PUBMED | CROSSREF

36. Mojumdar EH, Pham QD, Topgaard D, Sparr E. Skin hydration: interplay between molecular dynamics, structure and water uptake in the stratum corneum. Sci Rep 2017;7:15712.
    PUBMED | CROSSREF

37. Dai G, Freudenberger T, Zipper P, Melchior A, Grether-Beck S, Rabausch B, de Groot J, Twarock S, Hanenberg H, Homey B, et al. Chronic ultraviolet B irradiation causes loss of hyaluronic acid from mouse dermis because of down-regulation of hyaluronic acid synthases. Am J Pathol 2007;171:1451-61.
    PUBMED | CROSSREF

38. Yun MS, Kim C, Hwang JK. *Agastache rugosa* Kuntze attenuates UVB-induced photoaging in hairless mice through the regulation of MAPK/AP-1 and TGF-β/Smad pathways. J Microbiol Biotechnol 2019;29:1349-60.
    PUBMED | CROSSREF

39. Razia S, Park H, Shin E, Shim KS, Cho E, Kim SY. Effects of *Aloe vera* flower extract and its active constituent isoorientin on skin moisturization via regulating involucrin expression: *in vitro* and molecular docking studies. Molecules 2021;26:2626.
    PUBMED | CROSSREF

40. Lee HJ, Im AR, Kim SM, Kang HS, Lee JD, Chae S. The flavonoid hesperidin exerts anti-photoaging effect by downregulating matrix metalloproteinase (MMP)-9 expression via mitogen activated protein kinase (MAPK)-dependent signaling pathways. BMC Complement Altern Med 2018;18:39.
    PUBMED | CROSSREF

41. Park JE, Pyun HB, Woo SW, Jeong JH, Hwang JK. The protective effect of Kaempferia parviflora extract on UVB-induced skin photoaging in hairless mice. Photodermatol Photoimmunol Photomed 2014;30:237-45.
    PUBMED | CROSSREF

42. Han HS, Shin JS, Myung DB, Ahn HS, Lee SH, Kim HJ, Lee KT. *Hydrangea serrata* (Thunb.) Ser. extract attenuate UVB-induced photoaging through MAPK/AP-1 inactivation in human skin fibroblasts and hairless mice. Nutrients 2019;11:553.
    PUBMED | CROSSREF